*32nd EPS Conference on Plasma Phys. Tarragona, 27 June - 1 July 2005 ECA Vol.**29C**, O-3.005 (2005)*

Characterization of Multi-Temperature Fast Electron Beams on UHI Laser-Solid Interactions by Target Rear Side Self-Emission Diagnostics

J. J. Santos[1,2], M. Manclossi[1,3], A. Guemnie-Tafo[1], J. Faure[1], V. Malka[1], D. Batani[3]

[1] *Laboratoire d'Optique Appliquée, CNRS-ENSTA-Ecole Polytechnique, Palaiseau, France*

[2] *Centre Lasers Intenses et Applications, Univ. de Bordeaux 1-CNRS-CEA, Talence, France*

[3] *Dipartimento di Fisica "G. Occhialini", Univ. degli Studi di Milano-Bicocca, Milan, Italy*

In the intense laser-solid interactions, a relativistic and collimated supra-thermal electron current is injected from the plasma created on the region of the laser focal spot into the cold interior of the target. We report on results obtained at Laboratoire d'Optique Apliquée (LOA) from ultra-intense laser (up to a few $10^{20}\,\mathrm{Wcm}^{-2}$) interaction with Aluminium foil targets with thicknesses ranging from 10 to $100\,\mu$m. For these experiments, the delivered laser pulses, at 815 nm, are linearly polarized and can reach on-target energies up to 1.6 J in 40 fs (FWHM). The laser intensity contrast ratio was of the order of 10^{-7}.

The geometry and dynamics of the fast electron propagation has been investigated by means of the optical self-emission of the foils rear side, with spatial and spectral time-gated (5 ns) diagnostics. This radiation was collected on axis into the entrance slit of an optical spectrometer coupled to an ICCD camera (Fig. 1 shows a typical spectrum). The emitting zone was imaged on another ICCD camera, selecting two different wavelengths, $\lambda_{UV} = 405\,\mathrm{nm}$ and $\lambda_{Vis} = 546\,\mathrm{nm}$, with narrow-band interferometric filters ($\Delta\lambda \approx 10\,\mathrm{nm}$). The spectral sensitivity of both entire systems was established with an absolutely calibrated black-body radiation lamp. The goal of this work is to quantify the energetic and spatial characteristics of the generated fast electron population as well as the level of fast electron-induced heating.

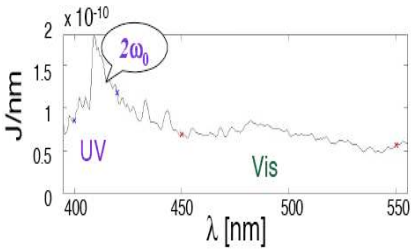

Figure 1: Time-gated spectrum of the rear of a $20\,\mu$m Al foil target.

The second harmonic of the laser light ($2\omega_0$) at 405 nm, is quite distinguishable from the surrounding broad spectrum in the visible region as presented on Fig. 1. As already seen in previous experiments [1, 2, 3], this coherent behaviour is ascribed to the micro-bunching of the relativistic electron flux through the targets. The required longitudinal modulation on the incident relativistic jet is associated with several collective accelerating mechanisms operating simultaneously, at relativistic intensities, on the laser focal spot near the critical density surface [3]. Vacuum heating and resonant absorption can drive electron bunches every laser field period ($\delta T = T_0 = 2\pi/\omega_0$). The $\boldsymbol{v} \times \boldsymbol{B}$ heating accelerates bunches every half period ($\delta T = T_0/2$).

When reaching the rear side of the targets and suddenly passing from the solid material into vacuum, each electron on the injected hot population will emit a spectrally-broad transition radiation. Provided the fast electron population remain periodically bunched after crossing a certain thickness of solid material, that radiation adds coherently for wavelengths close to $c\,\delta T$ and its harmonics (coherent transition radiation, CTR). The broad spectrum would correspond either to an incoherent emission (incoherent optical transition radiation, blackbody radiation) or to the foot of the $2\omega_0$ CTR spike.

In the left panel of Fig. 2 measurements of the emitted spectral densities scanning with the Aluminium target thickness are presented. They have been obtained for two spectral regions, a "UV" region around 405 nm (corresponding to the laser second harmonic) and a "visible" region around 546 nm (not related to any harmonic of the laser). The visible signal decreases faster with target thickness. In order to unveil the electron population responsible for the measured signals, we have to discriminate the dominant emission phenomena as a function of target thickness in the studied spectral range.

For target thicknesses larger than $75\,\mu$m we can fit the experimental data with the CTR produced by a periodically modulated relativistic electron flux. We use an analytical model which simulates a ballistic propagation of electron bunches injected at the front of different thickness layers [1, 3]. Assuming a $\boldsymbol{v}\times\boldsymbol{B}$ acceleration, the bunch injection is made at half the laser period $\delta T = T_0/2$, over the total laser pulse duration $\tau_0 \approx 40$ fs. This corresponds to the injection of $N_p = \tau_0/\delta T \approx 30$ bunches. An injection at $\delta T = T_0$ with $N_p \approx 15$ gives the same result. Each bunch is assumed to have both temporal and radial initial gaussian profiles with characteristic widths $\tau = T_0/10$ and $w_0 = 6\,\mu$m, the waist of the laser focal spot. The chosen duration of each bunch is based on PIC simulation results [3]. Taking into account a radial spreading of electrons during propagation, the width of the radial profile of the relativistic jet grows linearly with the foil thickness L, according to $w = 2L\tan\theta + w_0$. Here θ is the angular divergence half-angle, taken as a free parameter. Each bunch has an initial relativistic Maxwellian energy distribution with the temperature T_h, taken as the second free parameter. The total coherent spectral density of energy produced by the

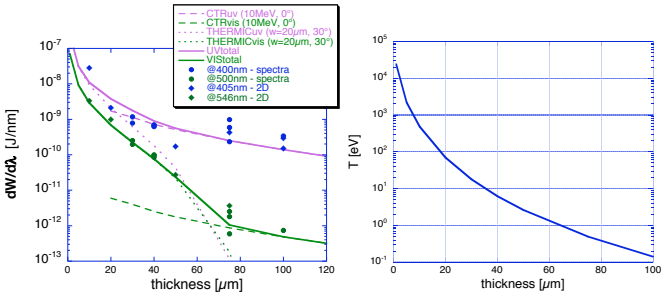

Figure 2: Left panel: Experimental spectral densities versus radiation models. Right panel: Expected Al foil electron temperatures.

N_p electron bunches is then given by the product of the emitted radiation by one electron by a factor, which takes into account the amount of charge radiating in phase:

$$\left.\frac{dW_{coh}}{d\lambda}\right|_{N_p\,\text{bunches}} = \left.\frac{dW_{OTR}}{d\lambda}\right|_{1\,e^-} P^2 \left|\tilde{\rho_L}(\omega)\right|^2 \left|\tilde{\rho_T}(k)\right|^2 \left(\frac{\sin(N_p\omega\delta T/2)}{\sin(\omega\delta T/2)}\right)^2 .$$

Here, P is the number of electrons per bunch, $\tilde{\rho_L}(\omega)$ and $\tilde{\rho_T}(k)$ are respectively the Fourier transforms of the longitudinal (i.e., temporal) and transverse profiles of each bunch, and the sinus cardinal corresponds to the interference between N_p bunches. This last term explains the formation of spectral lines for the harmonics of the electron injection period δT. The diminution of the $2\omega_0$ signal with target thickness, predicted by this model, is caused by both the growing radial size of the CTR formation region and mostly by the longitudinal broadening of each electron bunch due to the velocity dispersion, which progressively destroys the electron current modulation. Consequently, the coherent character of the emitted radiation is erased. This means that to ensure the emission of radiation in a coherent way for thick samples (intense $2\omega_0$ signals were still obtained for $L = 100\,\mu$m), the injected population must still conserve a certain modulation, that is, we need an electron population with a rather small velocity dispersion Δv. That is why we have established the following criterion for the coherent emission of radiation: $\Delta v \frac{L}{c} < \lambda_{obs}$, where λ_{obs} is the observed wavelength. Δv is highly sensitive on the electron temperature T_h. For a given initial temperature and divergence angle, this condition tells how the less relativistic electrons in each bunch have to be progressively abandoned in CTR modeling for growing target thickness, because they no longer satisfy the criterion on the velocity dispersion.

The experimental signals measured around 405 nm for targets thicker than 75 μm are well fitted for an electron population with a temperature of 10 MeV highly collimated ($\theta = 0°$). The $5-6\,10^8$ estimated total number of electrons involved in this emission corresponds to only a fraction of $5\,10^{-4}$ of the laser energy focused on target. Experimental signals at 546 nm, even if about 100 times weaker, are also well fitted by this model for the same parameters. This indicates that these signals correspond to the foot of the coherent spectral line emitted at $2\omega_0$.

Nevertheless, our CTR model does not describe the experimental data for the thinner targets, the discrepancy being quite flagrant in the "visible" region. We suppose that it is due to the blackbody radiation from the target, heated by the intense electron jet flux. For our working laser intensities and the expected electron energies, the resistive heating associated with the return current would be the main contributor. This return current is made from the free electrons of the target in order to neutralise the incident current. We developed a kinetic model which resolves the collective heating mechanism within the electron flux time-scale duration, according to the

following equation for the deposited energy per unit volume $\rho C_V \frac{d}{dt}(T_e[\mathrm{K}]) = \boldsymbol{E}\boldsymbol{j} = \frac{j^2}{\sigma}$.

The time-scale of only a few ps associated to this heating process allows us to neglect the process of thermal diffusion and expansion. That is why we considered constant the heating capacity of the medium $C_V = \frac{3}{2}K_B(n_e/\rho)$, where the plasma electron density is $n_e = Z^* n_i$, assuming the following values for the Aluminium conductivity $\sigma = 10^6\,\Omega^{-1}\mathrm{m}^{-1}$ and the degree of ionisation $Z^* = 6$. The expected maximum free electron temperatures are plotted in the right panel of Fig. 2 in function of target thickness. Since our acquisition time (5 ns) is much longer than the heating time, we have also to consider a cylindrically symmetric auto-similar expansion of the deposited energy reservoir. In order to estimate the blackbody radiation emitted during expansion, we integrated the Planck luminance over the experimental solid angle and the acquisition time window. The free parameters of our model are the temperature of the incident electron distribution T_h, their divergence angle θ and the initial injection zone of the fast electrons Φ_0. The best obtained fit for the experimental data was obtained for $\theta \approx 30^\circ$ and $\Phi_0 = 20\,\mu$m, which is larger than the laser focal spot w_0. The results were only slightly dependent on T_h, provided an laser energy into electrons conversion efficiency of 30%. Summing the modelled CTR and thermal emission, we managed to correctly fit all our experimental data (see full curve lines in the left panel of Fig 2).

In conclusion, the self-emission diagnostic is a powerful tool adequate for the characterisation of the fast electrons energy distribution and the dynamics of their transport through solid targets. The CTR produced by a micro-bunching of the incident relativistic current is highly sensitive to high electron energies and allowed to discriminate the hot tail of the laser-accelerated electron distribution as some highly collimated $5\,10^8$ electrons with a distribution temperature of 10 MeV. Besides, we deduced an important target heating due to the fast electron flux in thin targets and estimated a global fast-electron population with a total kinetic energy of about 30% of the on-target laser energy. These results are of capital interest within studies of the laser-production of energetic ion beams and the inertial confinement fusion fast ignitor.

The authors thank the LOA laser and technical staff for all the support during the experiments preparation and runs. They also aknowledge very fruitful discussions with V. Tikhonchuk, E. Lefevre, E. d'Humieres and L. Gremillet. The authors also thank O. Bernard from Andor Technology for lending two ICCD cameras.

References

[1] S. Baton *et al.* , Phys. Rev. Lett. **91**, 105001 (2003)

[2] J. Zheng *et al.* , Phys. Rev. Lett. **92**, 165001 (2004)

[3] H. Popescu *et al.* , Phys. of Plasmas **12**, 063106 (2005)